A Liver Level Set (LLS) Algorithm for Extracting Liver's Volume Containing Disconnected Regions Automatically

Puteri Suhaiza Sulaiman [β] Rahmita Wirza Rahmat [β] Ramlan Mahmod [β] Abd Hamid Abd Rashid [δ],

[β] *Faculty of Computer Science and Information Technology*
[δ] *Faculty of Medicine and Health Sciences*
Putra University of Malaysia, 43400 UPM Serdang, Selangor, Malaysia

Summary

In this paper a specified method is presented to facilitate segmentation of liver volume from CT images that contain disconnected regions automatically. The disconnected region appears because the physic of the liver containing multi-lobe structure, thus different lobe make different region in a single slice image. Most of the available liver segmentation algorithms that are based on gray level operation such as thresholding and active contour fail to extract the liver volume from these images automatically. Thus the core of the algorithm is a level set function that has the availability to manage separating and joining liver boundary routinely. The liver level set (LLS) is separated into two stages which a pre-processing stage and a level set with a hybrid energy minimization algorithm. The current slice is initialized by previous segmented liver boundary allowing changes in liver boundary topological changes to be inherited. The result show a respective segmentation with average 85% DCS when comparing with manual segmentation.

Key words:
image processing, liver segmentation, disconnected region, level set algorithm

1. Introduction

The first and foremost step in producing 3D liver visualization is liver volume segmentation. It aims in extracting the liver volume from CT/MRI dataset. Liver is considered as the most difficult organ to segment in abdominal area and even with radiologist assistants, extracting liver contour from each slice still a daunting tasks. The intricacy is cause by the liver's physic itself, since liver is made from soft tissues, there a large variation of liver geometry between patients. Plus, liver has similar tissues density with neighboring organ causing a limited contrast in CT/MRI gray level between them. Another frequently overlook feature of liver's physic is that the liver has a multi-lobe structure, thus different lobes can exhibit as disconnected regions in a transverse slice. Hence in the worst case scenario, liver may have more than two disconnected region with variation of shape in a single CT image as shown in figure 1.

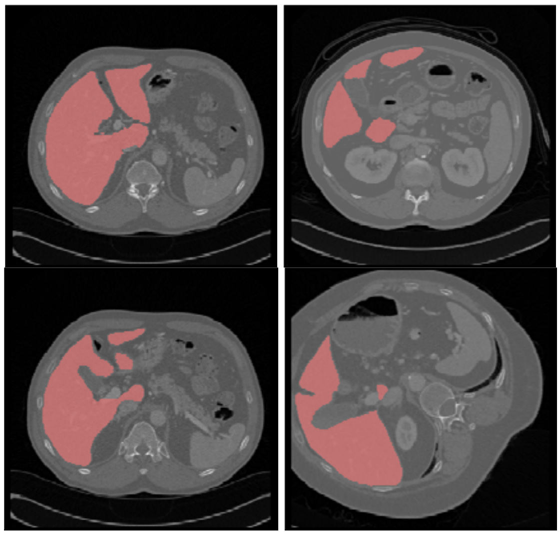

Figure 1: The disconnected region highlighted with red region

Earlier works on automatic liver segmentation are based on gray level image processing operation such as histogram analysis, thresholding, morphological operators and deformable contour model [1, 2, 3]. More recent works were also using multilevel thresholding and morphological filtering to get an initial liver contour, which then refined using active contour algorithm [4, 5, 6]. In these techniques, threshold values are very important and selecting the wrong values will cause a disconnected region to be removed. Plus the use of morphological filtering might reject separated liver region. Thus relaying solely on threshold value and morphological operators are not suitable for segmenting liver with several disconnected regions automatically.

To our knowledge, only Areste directly deals with liver disconnected region by doing a 3D region growing

Manuscript received December 5, 2008
Manuscript revised December 20, 2008

algorithm to obtain an initial segmentation of the liver [7]. This algorithm starts with a set of seed points and grows from it in a repeated fashion by appending to each seed its neighboring voxel that have similar intensities values. In order to ensure a successful segmentation of different lobes of the liver, a wide intensities range was used. This had caused the segmentation result to include artifacts from neighboring tissues. A 3d erosion operation and 2d region growing algorithm are then applied for each slice to further refine the liver contour. A major disadvantage of Areste's technique is it involved 2 layers of region growing algorithms, which can be both very consuming in processing time and memory.

Level set algorithm is a highly potential to carter disconnected region problem due to the ability of level set to handle merging and separating curve propagation. First attempt to segment the liver using level set is done by Pan et al [8]. He introduced an accumulative level-set speed function which varied by time to improve the detection sensitivity of weak edges. Plus, he also incorporated prior liver location based on anatomy knowledge to help in the segmentation process. Pan's 2D algorithm begins by initializing the curve through putting a small circle inside the liver region for each slice. Thus, if a disconnected region occurs in the current slice, a user needs to initialize a circle for each disconnected regions.

Lee advances the level set by predicting the initial liver shape using 2.5D shape propagation [9]. So instead of placing the curve in each slice, Lee's method required a manual input of seed points for each of the topmost and the bottommost liver slice. And if there are regions that are not connected from previous slice, additional seed points are needed.

Both attempts of using level set approach for liver segmentation required additional user interaction for disconnected regions [8, 9]. This does not fully utilize the benefits for using levels sets which able to carter the merging and separating propagating front. Thus, this paper aims in producing a liver level set (LLS) algorithm that can accurately segmented all disconnected liver regions automatically.

This paper is organized as follows. In section 2, described the basic of level set to give a background on the approaches that our algorithm is based on. Section 3 reveals our proposed LLS algorithms in details. In section 4 we discus the implementation and experimental result on our LLS algorithm. Finally in section 5, we present our concluding remarks, together with the benefits, drawback and future works.

2. Level Set Function

The level set idea was first introduced by Sethian and Osher in 1988 [10]. They model the propagating curve as a specific level set of a higher dimensional surface. Consider Ω to be a bounded open subset of $\Re^2$, with $\partial\Omega$ as its boundary. An image I can be defined as $I:\Omega \rightarrow \Re$. Now think about the evolving curve C in Ω, as the boundary of an open subset ω of Ω. With C is the boundary of $\omega(C=\partial\omega)$, we can defined the zero level set of a higher dimensional function ϕ as follows:

$$\phi(x,y,t=0)=\pm d \tag{1}$$

Where d is the distance from (x,y) to $\partial\omega$ at t = 0, and the plus minus sign is chosen if the point is outside or inside the subset ω. The evolution of the curve in its normal direction can be obtains by solving the partial differential equation given by Sethian and Osher [10]:

$$\frac{\partial\phi}{\partial t}=F|\nabla\phi| \quad \text{with} \quad \phi(x,y,0)=\phi_0(x,y) \tag{2}$$

Where the set $\{(x,y),\phi_0(x,y)=0\}$ defines the initial contour and F function is called the speed function, which specifies the speed at of the curve evolves along its normal direction. ϕ. The main advantage for this formulation is that $\phi(x,y,t)$ always remains a function as long as F is smooth. Therefore, as the surface ϕ evolves, the curve C may break, merge and change topology.

Another advantage is that the geometric properties of the curve are easily determined from a particular level set of the surface ϕ. For example, the normal vector for any point on the curve C is given by $\vec{n}=\nabla\phi$ and the curvature K is obtained from the divergence of the gradient of unit normal vector to the curve C given by

$$K=div\left(\frac{\nabla\phi}{|\nabla\phi|}\right)=\frac{\phi_{xx}\phi_y^2-2\phi_x\phi_y\phi_{xy}+\phi_{yy}\phi_x^2}{\left(\phi_x^2+\phi_y^2\right)^{\frac{3}{2}}} \tag{3}$$

2.1 Level Set with Gradient Edge Based Function

In image segmentation, the main goal is to formulate F function from the image to be segment. A general model for image segmentation given by Malladi [11] is defined as

$$F = g_I (F_0 - \varepsilon\kappa) \tag{4}$$

in which g_I is a term derived from the image itself. It is used to stop propagation of the contour near desired points such as points with high gradient or pre-specified intensity values. κ represents the curvature of the curve and acts as a regularization terms; F_0 is a constant; ε is a weighting parameter.

One example for g_I, is a gradient edge location function for an image I, given by the following formulation,

$$g_I = \frac{1}{1+|\nabla G_\sigma(x,y) * \mathrm{I}(x,y)|^2} \tag{5}$$

The edge based approach is suitable for images that have a high image gradient defining the edge. The disadvantage of above approach is that an initial curve must be put either inside or outside the object to be segment. Thus manual placement of initial curve usually is required in disconnected region, which fully prevent automatic segmentation [8, 9].

2.1 Level Set with Energy Minimization Based Function

Another way to halt the boundary evolution is by using an energy minimization approach. The advantage using energy minimization is the initial curve does not have to inside the object to be segments. Recalling that curve C can be viewed as the boundary of an open subset ω of Ω. Given that the region ω is *inside(C)* and the region ϖ is *outside(C)*, the Chan-Vese model can be used to stop the propagating curve [12]. Specifically, based on Chan-Vese, the energy, E, to be minimized is given by the following formulation,

$$E = \int_\omega (I-u)^2 dA + \int_\varpi (I-v)^2 dA \tag{6}$$

u and *v* represent the mean image intensities over ω and ϖ respectively. This energy is minimized when the mean image intensities in ω and ϖ are the most accurately approximated by *u* and *v*. This make it suitable for images that has weak edges and regions of piecewise constant intensities, which fits the characteristic in some of medical images. However, direct used of this model is not suitable for liver segmentation. This due to the fact that liver and the background i.e., other abdominal organs are not described accurately by mean intensities. This can lead to poor or incorrect segmentation. In order to successfully segment the liver using level set energy minimization approach, a new redefine energy to be minimized is needed.

Lankton et al. advanced Chan-Vese flow by proposing a hybrid evolution on energy minimization that took the advantages of both edge and region based contour which describe the energy as [13]

$$E = \oint_{C(s)} \int_{x\in\omega} (I\chi(x,s) - (u\ell(s))^2 \tag{7}$$
$$+ \int_{x\in\varpi} (I\chi(x,s) - v\ell(s))^2 ds$$

where $u\ell(s)$ and $v\ell(s)$ are the arithmetic means of points in local neighborhoods around the points, $C(s)$. The local neighborhood χ, is presented by a ball $B(C(s))$, with local interior is given by $\omega \cap \chi(x,s)$ and local exterior as $\varpi \cap \chi(x,s)$. The $\chi(x,s)$ function evaluates as 1 if a point *x* is inside the ball $B(C(s))$ centered about the point on the curve *C* specified by *s* and 0 otherwise. This combination allows curves deforming under this energy to find only significant local minima and delineate borders despite poor edge information and heterogeneous intensity profiles. This energy will be the foundation of our liver level set algorithm.

3. Liver Level Set Algorithm

The liver level set segmentation approach consists of two main steps: a pre-processing and a level set algorithm. The pre-processing involves a curve-based filtering which manipulates the image contrast to highlight the liver regions. The second stage begins by choosing a first initial slice which has the largest single liver regions in the input datasets. The first slice is then segmented to obtain an initial binary mask for the looping process. Since the input datasets are a series of connected slice images which are closely related to each other, an assumption is made, that a liver boundary in a slice is slightly different from its adjacent slice. This allows the use of the segmented liver boundary from the first initial liver slice as the initial binary mask for the next initial curve for liver boundary to be segmented. The advantage of doing this is to allow a smooth flow of boundary information between the slice images, thus, making it possible to segment disconnected region automatically. Figure 2 shows an overall flow diagram of the LLS algorithm.

Since the first initial slice will be in the middle of the input datasets, the looping process is done in two separate loops. The first loop start by comparing the current slice S_j number with the minimum slice number, *MinSlice*. If j is binger then *MinSlice*, then the next current slice will be S_{j-1} and the initial curve for hybrid energy minimization algorithm will be the binary mask M_k. This will continue until the value j is equal to *MinSlice*. Next the second loop start by comparing the current slice S_j number with the maximum slice number, *MaxSlice*. Similar with the first loop, if j is smaller then *MaxSlice*, then the next current slice will be S_{j+1} and the initial curve for hybrid energy minimization algorithm will be the binary mask M_k. This will also continue until the value j is equal to *MinSlice*, in which all the input datasets will be segmented.

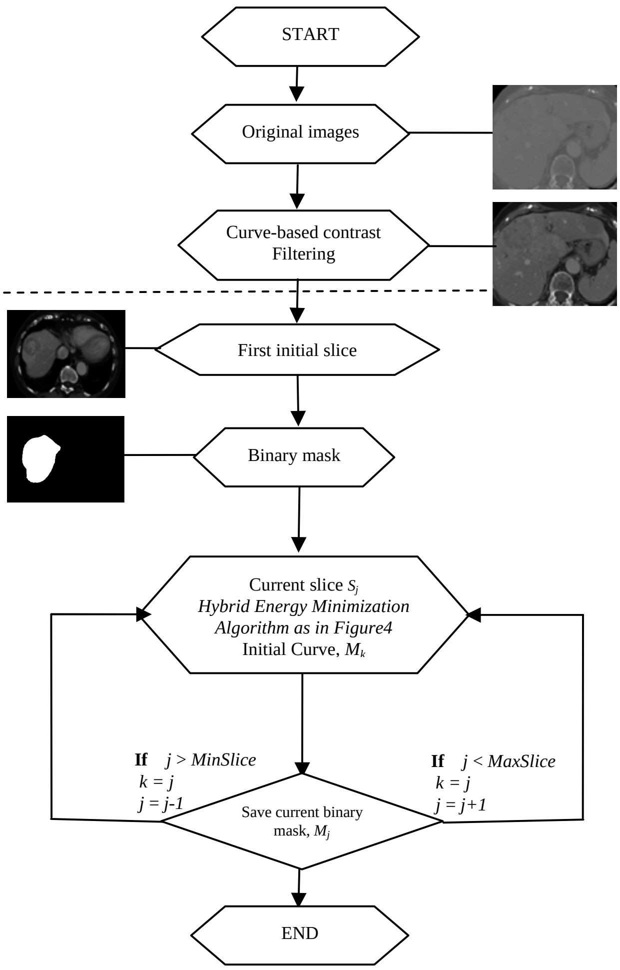

Figure 2: Flow diagram of the LLS algorithm.

3.1 Level Set with Gradient Edge Based Function

A pre-processing filter is applied to the original image in order to remove the noise from homogenous areas while highlighting the liver region in clear and sharp edges. Currently, this is done manually by the help of ITK-SNAP software. The ITK-SNAP offers a dynamic contrast adjustment that allows manipulation of multiple curve point as shown in figure 3.

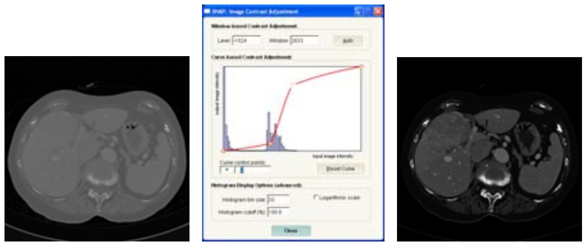

Figure 3: ITK snap image contrast adjustment printscreen (middle) for original liver image (right)
and result of the liver image (right)

3.2 LLS with Hybrid Energy Minimization

The LLS algorithm started with the hybrid energy presented in equation (7). This energy is being reformulated using level set framework where the evolving curve C is represented by zero level set of signed distance function ϕ as in (1). The interior region ω is defined by approximation of the smoothed Heaviside function as

$$\mathrm{H}\phi(x) = \begin{cases} 1, & \phi(x) < -\varepsilon \\ 0, & \phi(x) > \varepsilon \\ \frac{1}{2}\left\{1 + \frac{\phi}{\varepsilon} + \frac{1}{2}\sin\left(\frac{\pi\phi(x)}{\varepsilon}\right)\right\}, & otherwise \end{cases} \quad (8)$$

Likewise, the exterior region ϖ is define as $(1 - \mathrm{H}\phi(x))$. The derivative of $\mathrm{H}\phi(x)$ is used to specify the area just around the curve and can be presented as a smoothed version of the Dirac delta,

$$\delta\phi(x) = \begin{cases} 1, & \phi(x) = 0 \\ 0, & |\phi(x)| < \varepsilon \\ \frac{1}{2\varepsilon}\left\{1 + \cos\left(\frac{\pi\phi(x)}{\varepsilon}\right)\right\}, & otherwise \end{cases} \tag{9}$$

A local neighborhood χ function is being used as the mask for local interior and exterior regions [13]. A third parameter of the function χ is the radius *r* of the ball represented by *B(C(s))*. Noted that *r* remains constant in the implementation and is unrelated to any parameterization of the curve.

$$\chi(x,s) = \begin{cases} 1, & x \in B(C(s)) \\ 0, & otherwise \end{cases} \tag{10}$$

Therefore continuing with level set framework, the equation (6) of the hybrid energy, can be rewritten as

$$E = \oint_{\Omega} \mathrm{H}\phi(x)(I\chi(x,s) - u(s))^2 + (1 - \mathrm{H}\phi(x))(I\chi(x,s) - v(s)^2 d \tag{11}$$

Where *u(s)* and *v(s)* represent the local means of interior and exterior region respectively, and can be calculate by the following equations

$$u(s) = \frac{\int_{\Omega} \chi(x,s).\mathrm{H}\phi(x).I(x)dx}{\int_{\Omega} \chi(x,s).\mathrm{H}\phi(x)dx} \tag{12}$$

$$v(s) = \frac{\int_{\Omega} \chi(x,s).(1 - \mathrm{H}\phi(x)).I(x)dx}{\int_{\Omega} \chi(x,s).(1 - \mathrm{H}\phi(x))dx} \tag{13}$$

In order to obtain the evolution equation for ϕ, the derivative of E with respect to $\phi(y)$ is given as

$$\nabla_{\phi(x)} E = \delta\phi(x)((I(x) - u(s))^2 - (I(x) - v(s))^2 \tag{14}$$

Now we can deduce the Euler-Lagrange partial differential equation from (8). Parameterize the descent direction by t > 0, so the equation $\phi(x, y, t)$ for the curvature flow this hybrid energy is given by

$$\frac{\partial\phi}{\partial t}(x) = \delta\phi(x)\int_{\Omega}(I\chi(x,s)\delta\phi(s). \\ ((I(y) - u(s))^2 - ((I(y) - v(s))^2 dy \\ + \lambda\delta\phi(x) div\left(\frac{\nabla\phi(x)}{|\nabla\phi(x)|}\right) \tag{15}$$

Knowing ϕ^n, we must first compute $u(\phi^n)$ and $v(\phi^n)$ using (11) and (12) respectively. Then by using the curvature term terms *K*, directly to estimate ϕ^{n+1}

$$\frac{\phi^{n+1} - \phi^n}{\Delta t} = \delta\phi^n(x)\int_{\Omega}(I\chi(x,s)\delta\phi^n(s). \\ ((I(y) - u(\phi^n))^2 - ((I(y) \\ - v(\phi^n))^2 dy + \lambda\delta\phi^n(x)K \tag{16}$$

So the pseudo code hybrid energy minimization segmentation algorithm can be seen in figure 4 below.

```
n = 0
Initialize φ by φ^n
For n=1 to max do
    Compute u(φ^n) and v(φ^n) by (12) and (13)
    Compute curvature term K by (3)
    Compute φ^{n+1} by (16)
```

Figure 4: Hybrid energy minimization algorithm

4. Experiment and Result

4.1 Experiment

An experiment had been conducted on 7 abdominal CT scan dataset. Each dataset contain livers various sizes, shape and may contain more than one disconnected regions. The algorithm was initialized by selecting the first initial slice that contain a single liver region, preferred the largest region that contain all relevant information such as the veins and tumor inside it. This allows the algorithm to include all this information as part of the liver. User must include information on the slice number for the starting of liver region as *MinSlice* and the end of liver region as *MaxSlice*.

Choosing the right *r* value is also very important because during the experiment, a bigger we found that a large *r* value will cause the liver boundary to leaks other organ especially the muscle around the rib area. However choosing a smaller *r* value, has cost liver boundary to expand or shrink slowly, therefore needs more iteration time. This eventually leads to failing to capture far liver region. Thus by experimenting with various size of *r* value, we found that the most suitable value is around 10 to 20 pixels depending on size and boundary of liver images.

4.2 Result

The gold standard for automatic segmentation is to compare the result with manual segmentation made by an expert. For this we calculate the liver volume overlapping using dice similarity coefficient (DSC), the false positive ration\ (FPR) and false negative ratio (FNR) given by the following

$$DSC = \frac{2(M_l \cap A_l)}{M_l + A_l}; FPR = \frac{2(M_b \cap A_l)}{M_l + A_l}; FNR = \frac{2(M_l \cap A_b)}{M_l + A_l} \quad (17)$$

where A and M represent respectively the automatic and manual segmentation and l and b correspond respectively to the consideration of liver and background pixels. Table 1 shows the result for each patient with their number of disconnected regions. From observation, the number of disconnected region has an impact to the DCS percentage, in which the smaller numbers of disconnected regions give a higher DSC percentage. However, using the LLS algorithm, all the disconnected regions are segmented successfully with an average DSC percentage of 85.54. Furthermore the average percentage of FNR and FPR under 5% is considered as a good error ratio. A balance between FNR and FPR needs to be found because the two error ratios are interdependent and evolve in an opposition manner. For liver segmentation the objective is have both low FNR and FPR.

Table 1: Result of Liver Segmentation using the LLS algorithm

Patient	# Disconnected Region	DSC [%]	FNR [%]	FPR [%]
1	2	87.98	3.45	4.19
2	3	82.45	4.36	7.55
3	5	79.78	5.93	6.24
4	1	91.43	0.93	3.5
5	2	81.74	5.77	5.07
6	3	85.82	4.05	4.59
7	2	89.12	2.45	5.8
8	2	92.55	1.22	0.98
9	4	79.03	7.4	6.7
	average	85.54	3.95	4.96
	stdard derivation	4.74	2.07	1.85

Figure 5 shows a sequence of liver images taken from patient 1 containing two disconnected regions. The green contour represent the initial curve for the current image taken from previous slice, segmented liver boundary. The red contour represents the final segmented of liver boundary for the current image. From this figure, we can see how the topology changes can be inherited by the next image, thus allowing liver boundary to be separated into two disconnected region using our LLS algorithm.

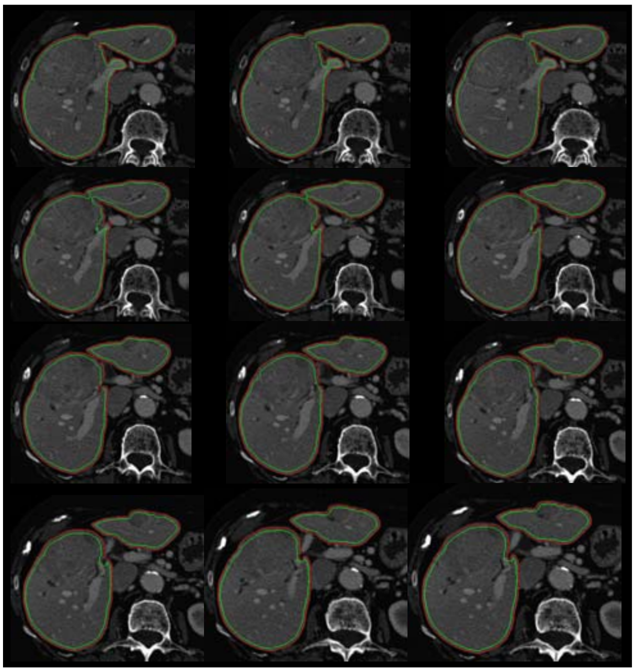

Figure 5: Sequence of liver boundary images with the initial curve (green contour) final liver boundary (red contour).

5. Conclusion

In this paper, a LLS algorithm for segmenting disconnected liver region was proposed. The LLS algorithm is based from a hybrid energy minimization formulation. The hybrid energy is reformulate in level set framework in a looping manner, thus allowing to inherent the topology changes from previous image. By using the previous segmented liver boundary as the initial curve slice for the slice, the disconnected regions are being segmented automatically.

Based on the experiment conducted on nine different patients that had various disconnected region images, we found that using LLS algorithm, we are able to extract all this disconnected region successfully and automatically.

However he limitation for the hybrid energy is that the segmented result is dependable on the size of radius *r* of the ball *B(C(s)).* If r is too small, the LLS algorithm fails include far liver region and if the *r* value is too big it will nearby artifacts causing a false segmentation. Thus for the future works, an automatic generation of r value based on anatomy of the liver is highly recommended.

References

[1] Bae, K.T., et al.: Automatic segmentation of liver structure in ct images. Med. Phys. 20 (1993)

[2] Gao, L., et al.: Automatic liver segmentation technique for three-dimensional visualizationof ct data. Radiology 201, 359–364 (1996)

[3] Kobashi, M., Shapiro, L.: Knowledge-based organ identification from ct images. Pattern Recognition 28 (4), 475–491 (1995)

[4] Lim, S.J., et al.: Automatic segmentation of the liver in ct images using the watershed algorithm based on morphological filtering. In: Proceedings of SPIE, vol. 5370, pp. 1658–1666 (2004)

[5] Lim, S.J., et al.: Segmentation of the liver using the deformable contour method on ct images. In: Proceedings of SPIE, vol. 3767, pp. 570–581 (2005)

[6] Lim, S.J., et al.: Automatic liver segmentation for volume measurement in ct images. Journal of Visual Communication and Image Representation 17(4), 860–875 (2006)

[7] Areste, R. and Yang, Y.Y. and Hsieh, J.: An Image Enhancement Procedure for 3D Visualization of Liver CT Data. IEEE Southwest Symposium, 153-167 (2006)

[8] Pan, S., and Dawant, B. M. : Automatic 3D Segmentation of the liver from abdominal CT images: a level-set approach. In: Proceeding of SPIE, vol. 4322 pp. 128-138 (2001)

[9] Lee, J., et al. Efficient liver segmentation exploiting level set speed images with 2.5D shape propagation. In: 3D Segmentation in the Clinic: A grand Challenge, pp. 189-196 (2007)

[10] Sethian, J. A. Level set methods and fast marching methods: Envolving interfaces. In: Computational Geometry, Fluid Mechanics, Computer Vision and Materials Science. Cambrige University Press (1999)

[11] Malladi, R., Sethian, J. A., and Vemuri, B. Shape Modelling with front propagation: A level set approach. In IEEE Trans. on Pattern Analysis and Machine Intelligence, 7(2). Pp. 158-174 (1995)

[12] Chan, T. and Vese, L. Active contours without edges. In IEEE Trans. Image Processing, 10(2). Pp. 266-277. (2001)

[13] Lankton, S. et al. Hybrid Geodesic Region-Based Curve Evolutions for Image Segmentation. In Proceedings of SPIE Medical Imaging (2007)

Puteri Suhaiza Sulaiman is a phd candidate at Faculty of Computer Science and Information Technology, UPM, Malaysia. Her research study is focusing on liver image segmentation and 3D liver visualization.

Rahmita Wirza Rahmat PHD is currently an Associate Professor and the head department of multimedia at Faculty of Computer Science and Information Technology, Putra University of Malaysia. Her research interest include image processing, medical visualization and reverse engineering.

Ramlan Mahmod PHD is currently an Associate Professor at Faculty of Computer Science and Information Technology, Putra University of Malaysia. His research interest includes image processing, artificial intelligence and security computing.

Abdul Hamid Abdul Rashid PHD is currently an Professor at Faculty of Medicine and Health Sciences, Putra University of Malaysia. His fields of specialization comprises of Anatomy: Macroscopic, microscopic, neuroanatomy, developmental anatomy.